

Temperature-driven meltwater production and hydrochemical variations at a glaciated alpine karst aquifer: implication for the atmospheric CO₂ sink under global warming

Cheng Zeng · Vivian Gremaud · Haitao Zeng ·
Zaihua Liu · Nico Goldscheider

Received: 12 January 2011 / Accepted: 20 June 2011 / Published online: 8 July 2011
© Springer-Verlag 2011

Abstract About two hydrological years of continuous data of discharge, temperature, electrical conductivity and pH have been recorded at the Glarey spring in the Tsanfleuron glaciated karst area in the Swiss Alps, to understand how glaciated karst aquifer systems respond hydrochemically to diurnal and seasonal recharge variations, and how calcite dissolution by glacial meltwater contributes to the atmospheric CO₂ sink. A thermodynamic model was used to link the continuous data to monthly water quality data allowing the calculation of CO₂ partial pressures and calcite saturation indexes. The results show diurnal and seasonal hydrochemical variations controlled chiefly by air temperature, the latter influencing karst aquifer recharge by ice and snowmelt. Karst process-related atmospheric CO₂ sinks were more than four times higher in the melting season than those in the freezing season. This finding has implication for understanding the atmospheric CO₂ sink in glaciated carbonate rock terrains: the carbon sink will

increase with increasing runoff caused by global warming, i.e., carbonate weathering provides a negative feedback for anthropogenic CO₂ release. However, this is a transient regulation effect that is most efficient when glacial meltwater production is highest, which in turn depends on the future climatic evolution.

Keywords Hydrochemical variation · Glaciated karst aquifer · Temperature-controlled recharge · Karst process · Atmospheric CO₂ sink · Switzerland · Alps

Introduction

The balance between terrestrial chemical weathering of rocks and marine carbonate precipitation is an important control on CO₂ concentration in the atmosphere (Holland 1978). Gibbs and Kump (1994) simulated the atmospheric CO₂ concentrations at the last glacial maximum and demonstrated that chemical weathering has a major effect on atmospheric CO₂ concentrations. Chemical denudation rates in catchments containing small valley glaciers are 1.2–2.6 times higher than the continental average (Sharp et al. 1995). This is attributed to high water fluxes and intense rock–water interactions, facilitated by reactive, freshly comminuted, silt and clay-sized particles (Anderson et al. 1997; Tranter et al. 1993).

According to Liu et al. (2010), the global water cycle is an important sink for atmospheric CO₂ in the form of dissolved inorganic carbon (DIC). This sink may increase with intensified water circulation resulting from global warming. Large volumes of glacier ice and “permanent snow” will go into the water cycle, so there is a tremendous potential for increased chemical weathering and CO₂ uptake. However, to date, there are no systematic studies

C. Zeng · H. Zeng · Z. Liu (✉)
State Key Laboratory of Environmental Geochemistry,
Institute of Geochemistry, Chinese Academy of Sciences,
Guiyang 550002, China
e-mail: liuzaihua@vip.gyig.ac.cn

V. Gremaud
Centre of Hydrogeology, University of Neuchâtel,
2009 Neuchâtel, Switzerland

N. Goldscheider (✉)
Division of Hydrogeology,
Karlsruhe Institute of Technology (KIT),
Institute of Applied Geosciences (AGW),
Kaiserstr. 12, Karlsruhe 76131, Germany
e-mail: goldscheider@kit.edu

investigating and quantifying the expected increase of the atmospheric CO₂ sink by chemical carbonate weathering (i.e., karstification) in alpine karst areas covered by glaciers and snow.

Therefore, an extensive study program was established at the Tsanfleuron glaciated karst area in the Swiss Alps. The study included continuous monitoring of discharge, water temperature, specific electrical conductivity (EC) and pH at the Glarey spring, the main spring draining this aquifer system. The primary study objective was to understand how glaciated karst aquifer systems respond hydrochemically to recharge at seasonal and diurnal time scales, and how the glacier meltwater contributes to the atmospheric CO₂ sink. To our knowledge, this is the first study investigating the atmospheric CO₂ sink in a glaciated karst area with high-resolution monitoring of temporal hydrochemical variations.

Theoretical background

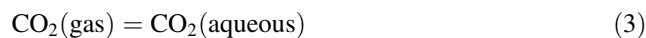
The two key parameters for the quantification of the carbonate weathering-related atmospheric CO₂ sink are DIC and discharge (Liu et al. 2010). However, DIC cannot be measured directly and continuously but has to be deduced from other data, using theoretical considerations. The CO₂ partial pressure (pCO₂) and the calcite saturation index (SI_c) of spring water are related to Ca²⁺ and HCO₃⁻ concentrations, pH and water temperature (Liu et al. 2004, 2007). At karst springs, discharge, temperature, electrical conductivity (EC) and pH can relatively easily be recorded continuously, using measurement probes and data loggers. Detailed hydrochemical spring water characteristics can usually be obtained from the analysis of a limited number of water samples in the laboratory. Combining the two data sets makes it possible to set up empirical relations between continuous physicochemical data and water chemistry. In most limestone areas, including glaciated and alpine karst systems, calcite dissolution determines the spring water composition (Fairchild et al. 1994, 1999). Therefore, Ca²⁺ and HCO₃⁻ are the dominant ions and their concentrations can be deduced from continuous EC data. When concomitant pH measurements are available, the CO₂ partial pressure in the water under equilibrium conditions can be calculated as follows:

$$p\text{CO}_2 = \frac{(\text{HCO}_3^-)(\text{H}^+)}{K_{\text{H}}K_1} \quad (1)$$

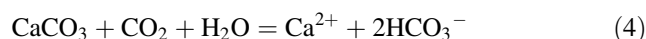
where parentheses denote species activity in mol/L, K_{H} is Henry's law constant, and K_1 is the first dissociation constants for CO₂ in water (both constants are temperature dependent). The calcite saturation index can finally be determined as follows:

$$\text{SI}_c = \log \left(\frac{(\text{Ca}^{2+})(\text{CO}_3^{2-})}{K_c} \right) \quad (2)$$

where K_c is the temperature-dependent equilibrium constant for calcite (Stumm and Morgan 1981; Drever 1988). $\text{SI}_c > 0 \pm 0.1$ means that the water is supersaturated with respect to calcite, whereas $\text{SI}_c < 0 \pm 0.1$ indicates undersaturation and thus the potential for limestone dissolution. Karst processes draw CO₂ out of the atmosphere. The first step is diffusion of CO₂ gas into solution:



The second step is the acid hydrolysis of calcite:



In glaciated karst areas, these processes are thought to occur in subglacial and periglacial drainage channels that allow gas exchange with the atmosphere (Brown et al. 1994). According to Liu et al. (2010), the carbonate weathering-related carbon sink can be calculated as:

$$\text{Carbon sink} = 0.5 \times Q \times [\text{HCO}_3^-] \quad (5)$$

where Q is discharge and square brackets indicate concentrations. The factor 0.5 results from the fact that only half of the HCO₃⁻ in the water originates from atmospheric CO₂, while the other half comes from the hydration of carbonate in calcite. While Eq. 5 is easily applicable to hydrogeological systems with relatively stable discharge and hydrochemical conditions, the application to glaciated alpine karst systems with strong diurnal and seasonal variations is challenging.

Test site and methods

Geological and hydrological setting

The Tsanfleuron–Sanetsch area is located in the southwestern Swiss Alps. It consists of a karst aquifer drained by the Glarey spring at its lowest point (1,553 m) and overlain by the rapidly retreating Tsanfleuron glacier in its upper part, from ca. 2,550 to 3,000 m (Fig. 1).

Geologically, the test site belongs to the Helvetic zone and is formed by the Diablerets nappe. The stratigraphy includes Jurassic, Cretaceous and Paleogene sedimentary rocks, mainly marl and limestone (Fig. 2). The Cretaceous Urgonian Limestone, also known as *Schrattenkalk*, is arguably the most important karstifiable formation of the Alps (Goldscheider 2005). In the study area, it forms impressive karrenfields, together with the overlying Eocene limestone. Glacier-polished surfaces predominate at higher altitudes, between the end moraine from 1,855/1,860 (“Little Ice Age”) and the recent glacier front. Speleological



Fig. 1 Impression of the retreating Tsanfleuron glacier that directly overlies and recharges a karst aquifer. The polished limestone surfaces in its forefield are partly covered by moraine (Photo: N. Goldscheider)

observations and tracer test results indicate that the two limestone formations form one hydraulically connected Urgonian–Eocene karst aquifer (Gremaud et al. 2009).

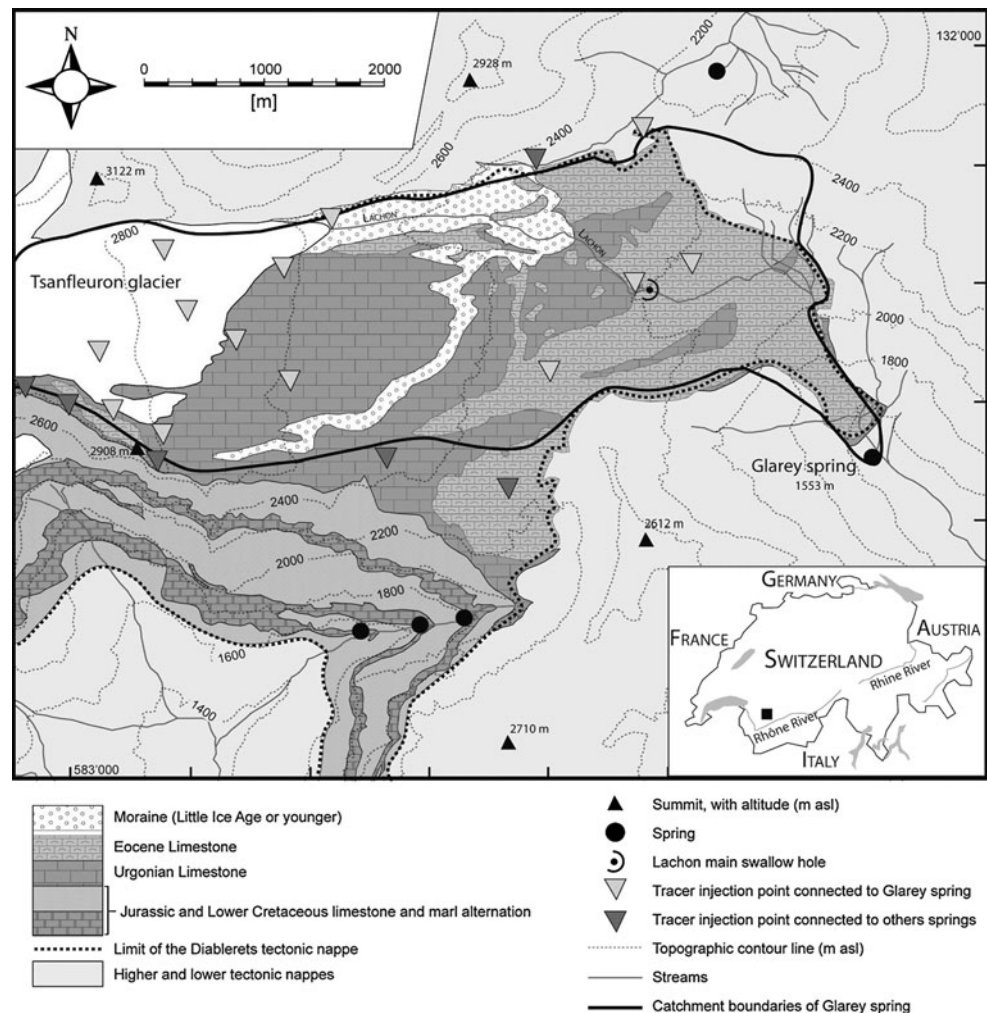
The hydrological regime of the area can be subdivided into three characteristic periods: during the snow cover period (or freezing season), typically lasting from November to April, most precipitation falls as snow and the area is mostly covered by ca. 1–3 m of snow. The snowmelt period often begins in April and creates transient streams at the surface of the karrenfields that sink underground via swallow holes, but most of the meltwater directly infiltrates into the aquifer underneath the snowpack. By mid-July, the snowline typically reaches the glacier front. This is the beginning of the ice melt period, which typically lasts until October or sometimes November. The snowmelt and ice melt can be grouped as melting season. In warm and dry summers, such as 2003, the snowline rises above the highest point of the glacier, i.e., the entire glacier forms one large ablation zone, which means that this glacier will vanish under similar or even warmer climatic conditions.

During the ice melt period, the glacier becomes the main source of aquifer recharge. Three recharge processes have been identified and confirmed by means of tracer tests (Gremaud and Goldscheider 2010): (1) supraglacial streams sinking into the glacier via moulines, as well as subglacial meltwater streams, infiltrate into the aquifer

underneath the glacier; (2) numerous supraglacial and subglacial meltwater streams emerging along the glacier front flow over limestone for several tens of meters before sinking into the aquifer via swallow holes and open fractures; (3) the main glacier stream (Lachon) that has its source at the glacier mouth, flows several kilometers over moraine before sinking into swallow holes in the centre of the karrenfields. All these recharge processes display strong diurnal and seasonal variations and also change from year to year as a function of glacier retreat.

Five relevant springs drain the Tsanfleuron region (Fig. 2), but tracer tests have demonstrated that most of the glacier and karrenfields (ca. 11 km²) belong to the catchment of the Glarey spring that consists of two orifices: the lower, permanent orifice at 1,553 m a.s.l. was formed by means of a 30-m long artificial drainage gallery and used for the drinking water supply for the community of Conthey, and for irrigation. When the discharge of this permanent spring exceeds 40 L/s, a nearby overflow (ca. 15 m higher) becomes active. Numerous tracer tests and hydrochemical data have shown that water from the overflow and from the permanent spring are identical. They are consequently treated as one spring. The total discharge of Glarey spring varies from ca. 35 L/s in winter up to more than 2,000 L/s during snowmelt and storm rainfall periods (Gremaud et al. 2009; Gremaud and Goldscheider 2010). All data and analyses concerning Glarey spring presented

Fig. 2 Generalized geological map of the Tsanfleuron area, which belongs to the Diablerets nappe and mainly consist of Urgonian Limestone. The stratigraphy of the over- and underlying tectonic nappes has been simplified. Relevant springs and streams are also shown (after Gremaud et al. 2009)



and discussed here below always refer to the total spring (i.e., drinking water spring + overflow spring).

Monitoring of hydrological, physicochemical and chemical parameters

Precipitation and temperature: two tipping-bucket rain gauges with a temporal resolution of 30 min were installed near the glacier (2,580 m) and at the eastern margin of the karrenfields (2,120 m). The latter of these stations also recorded air temperature. Additional temperature data were obtained from a MeteoSwiss weather station near the top of the glacier (2,966 m).

Discharge (Q): at the Glarey drinking water spring, discharge was continuously recorded at a weir equipped with an ultrasonic water level device and a pressure probe. At the overflow spring, a pressure probe was installed. The stage–discharge curves were obtained by flow measurements using the salt-dilution method.

Physicochemical parameters: specific electric conductivity (EC) was measured using a field conductivity probe

(WTW 340i, Weilheim, Germany) with an accuracy of $0.5 \mu\text{S}/\text{cm}$; the probe also measures water temperature (T) with an accuracy of 0.1°C . A pH probe (WQ201, Global Water Instrumentation, Gold River, California, USA) connected to a data logger (DT50, DataTaker, Orbatex, Grenchen, Switzerland) was also installed at the Glarey spring.

Major ion chemistry: for this study, 162 water samples from the Glarey spring and 53 samples from other springs, glacial streams and swallow holes were analyzed in the CHYN laboratory. Major ions were measured by means of ion chromatography (IC, Dionex DX-120) for the cations, sodium (Na^+), potassium (K^+), magnesium (Mg^{2+}) and calcium (Ca^{2+}), and anions: chloride (Cl^-), nitrate (NO_3^-) and sulfate (SO_4^{2-}). Bicarbonate (HCO_3^-) was measured using an automatic acid–base titration instrument.

CO_2 partial pressures and calcite saturation indices were calculated as described above (theoretical background), using the old but still valid software WATSPEC (Wigley 1977).

Results

General hydrochemical spring water characteristics and empirical relations

Table 1 shows the general hydrological and chemical characteristics of Glarey spring during the melting season, in July 2007. Discharge varies between 752 and 1,628 L/s, EC is within a range of 130–144 μS/cm, and water temperature is 3.69–3.88°C. Calcium and bicarbonate are the dominant ions, with mean concentrations of 23.3 and 77.4 mg/L, respectively. Sulfate is also relevant (4.4 mg/L) and mainly originates from the oxidation of sulfide minerals (Fairchild et al. 1999). All other ions occur in very low concentrations. Lower discharge but higher concentrations of all ions have been observed in winter (also shown in Table 1).

Combining the obtained long-term data sets of EC (continuously recorded in the field) and all water chemistry data (selected water samples measured in the laboratory) from the Glarey spring allowed the following empirical relations to be established:

$$[Ca^{2+}] = 0.162EC + 4.362, \quad r = 0.84$$

$$[HCO_3^-] = 0.488EC + 18.234, \quad r = 0.86$$

$$[SO_4^{2-}] = 0.934e^{0.0113EC}, \quad r = 0.95$$

where brackets denote species concentrations in mg/L, and EC is in μS/cm at 25°C. These relations were used to generate data series of calcium, bicarbonate and sulfate concentrations, which were then used as input parameters for WATSPEC for the calculation of pCO₂ and SIc, along with temperature and pH data. For all other ions, which only occur in very low concentrations (Table 1), mean values were used as input parameters (Liu et al. 2004, 2007).

Diurnal hydrochemical variations during the melting seasons

Figure 3 shows the observed variations at Glarey spring during 5 days in July 2007, along with the calculated atmospheric CO₂ sink, based on the data presented in Table 1. EC is roughly reverse to spring discharge, but the discharge maximum occurs 5 h before the EC minimum, indicating a combination of piston flow and dilution effect. The discharge maximum is partly caused by pressure transfer in the aquifer, while the EC minimum indicates the physical arrival of freshly infiltrated glacial meltwater. Variations of Ca²⁺, HCO₃⁻, SO₄²⁻ and other ions are parallel to EC, illustrating the empirical relations presented above. Variations of water temperature are small, indicating the thermal buffering capacity of the system, i.e., variable temperatures of infiltrating meltwaters are equalized inside the karst aquifer.

The calculated HCO₃⁻ fluxes and the atmospheric CO₂ sink display diurnal variations parallel to discharge, with maximum values during peak flows at around 8 p.m. This means that the effect of higher discharge outweighs the effect of lower HCO₃⁻ concentrations by dilution.

Seasonal variations

The Glarey spring shows strong seasonal hydrological and hydrochemical variations that also result in substantial variations of the calculated SIc, pCO₂ and carbon sink (Table 2, Fig. 4). Air temperatures measured on top of the glacier (2,966 m) vary between -20.3°C (freezing season) and +12.8°C (melting season), resulting in highly variable spring discharge from 35 to 2,145 L/s. The calculated bicarbonate concentrations (deduced from EC) also display

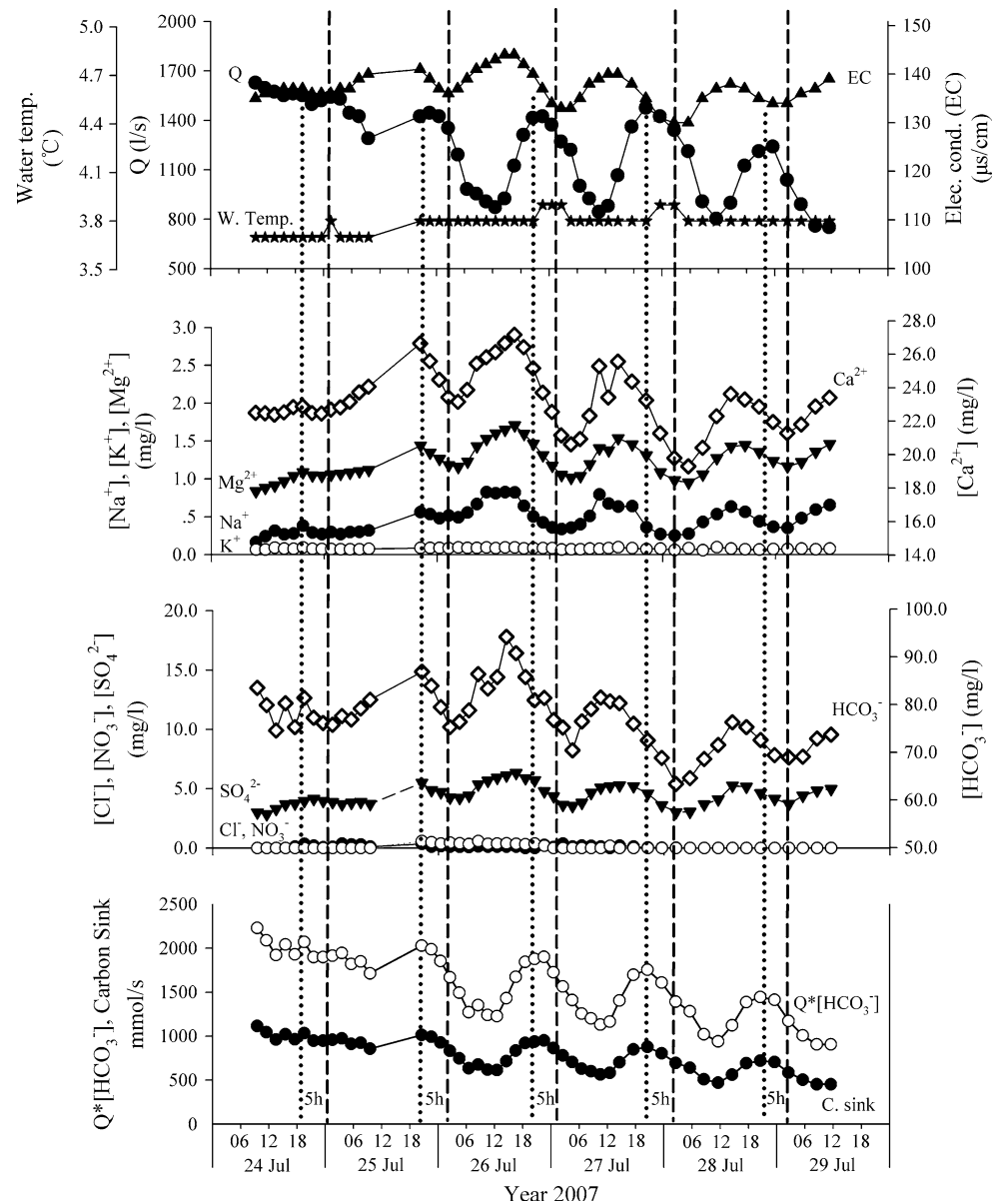
Table 1 Statistics on discharge, physicochemical parameters and major ion chemistry of Glarey spring during the melting season (July 2007)

	Discharge (L s ⁻¹)	Water T (°C)	EC (μS cm ⁻¹)	Na ⁺ (mg L ⁻¹)	K ⁺ (mg L ⁻¹)	Mg ²⁺ (mg L ⁻¹)	Ca ²⁺ (mg L ⁻¹)	Cl ⁻ (mg L ⁻¹)	NO ₃ ⁻ (mg L ⁻¹)	SO ₄ ²⁻ (mg L ⁻¹)	HCO ₃ ⁻ (mg L ⁻¹)
N	50	50	50	50	50	50	50	50	50	50	50
Minimum	752	3.69	130	0.16	0.06	0.84	19.30	0.00	0.00	2.83	63.32
Maximum	1,628	3.88	144	0.82	0.10	1.71	27.18	0.36	0.56	6.32	94.18
ED	877	0.19	14	0.66	0.04	0.87	7.88	0.36	0.56	3.50	30.87
Mean	1,230	3.78	137	0.46	0.08	1.23	23.29	0.10	0.11	4.42	77.42
SD	265	0.05	3	0.18	0.01	0.22	1.82	0.11	0.18	0.88	6.27
CV	0.22	N/A	0.02	0.39	0.13	0.18	0.08	1.13	1.63	0.20	0.08
13 January 2008	40	4.10	329	4.09	0.33	6.99	65.1	0.14	0.62	33.2	189.2
27 February 2008	597	4.60	281	1.98	0.16	4.05	55.6	0.73	0.43	13.7	161.5

Selected results from the freezing season are indicated for comparison

T temperature, EC electrical conductivity, N number of samples, ED extreme difference (=max - min), SD standard deviation, CV coefficient of variation (=SD/mean), N/A not applicable

Fig. 3 A 5-day time series of discharge (Q), water temperature, electrical conductivity (EC), concentrations of major ions, $Q[\text{HCO}_3^-]$ and carbon sink observed at Glarey spring, 24–29 July 2007. Marked diurnal cycles are found, where water temperature variations are small, EC and major ion concentrations show anti-phase change with Q (about 5-h lag time), while carbon sink shows in-phase change with Q



large variations. Figure 4 shows that the lowest EC levels, and thus the lowest bicarbonate concentrations, occur in the melting season (dilution effect), while much higher concentrations can be observed during the freezing season. However, the higher flow rates during the melting season override the effect of lower concentrations, so that the calculated carbon sink is substantially higher in the melting season than in the freezing season.

Detailed analysis of the freezing and melting seasons

In winter, the area is mostly covered by snow, and temperatures often remain below freezing point for several weeks. Figure 5 shows data from 3 days in January 2008. Air temperatures measured on top of the glacier at 2,966 m

vary between ca. -6.5°C during day and -10°C at night. As a result, Glarey spring displays no significant diurnal variations. Discharge is near its annual minimum and slowly decreases from ca. 39.0 to 37.5 L/s. Observed variations of water temperature, EC and pH are insignificant, such as the calculated variations of CO_2 partial pressure and calcite saturation index. The calculated carbon sink slowly decreases from ca. 61 to 58 mmol/s largely parallel to spring discharge.

Table 3 presents a detailed statistical analysis of the entire freezing season, from 1 November 2007 to 15 April 2008, although snowmelt in the lower parts of the area already starts at that time of the year. During the freezing season, the mean spring discharge is 118 L/s (lower than the annual average) and the mean bicarbonate concentration is

Table 2 Statistics on the seasonal hydrological and hydrochemical variability observed at Glarey spring during one hydrological year (1 November 2007 through 31 October 2008)

	Air <i>T</i> (°C)	Discharge (L s ⁻¹)	Water <i>T</i> (°C)	EC (μS cm ⁻¹)	[Ca ²⁺] (mg L ⁻¹)	[HCO ₃ ⁻] (mg L ⁻¹)	pH	SI _C	pCO ₂ (Pa)	Carbon sink (mmol s ⁻¹)
<i>N</i>	8,784	13,915	13,915	13,915	13,915	13,915	11,646	11,646	11,646	13,915
Minimum	-20.3	35	3.68	38 ^a	10.5 ^a	36.8 ^a	7.66	-0.96	13.0 ^a	50
Maximum	12.8	2,145	4.70	349	61.0	188.7	8.53	0.46	260.6	1,583
ED	33.1	2,110	1.02	311	50.5	151.9	0.86	1.42	247.6	1,533
Mean	-2.2	610	4.21	227	41.3	129.3	8.07	0.01	87.6	462
SD	6.1	557	0.23	90	14.7	44.1	0.11	0.30	39.7	341
CV	N/A	0.91	0.06	0.40	0.35	0.34	0.01	N/A	0.45	0.74

Legends see Table 1

^a Outliers

173.8 mg/L (higher than the annual average; see Table 2). This results in a mean carbon sink of 161 mmol/s during freezing season, i.e., substantially lower than the annual mean value of 462 mmol/s. The absolute annual carbon sink minimum (50 mmol/s) also occurs in the freezing season, during the period of minimum spring discharge. These findings confirm that the effect of lower spring discharge overrides the effect of higher bicarbonate concentration. The coefficient of variation (CV) is 0.22 for discharge, but only 0.08 for HCO₃⁻ (Table 1). This also shows that discharge has a higher impact on the calculation of the carbon sink.

A different pattern was observed during the melting season. Figure 6 shows 3 days of data from September 2007, when temperature-induced variability of glacial meltwater production resulted in marked diurnal variations monitored at Glarey spring. Air temperatures measured at 2,966 m ranged between 2 and 8°C, with maximum values around noon. The highest meltwater production occurred around 2 p.m. (not monitored continuously), while spring discharge reached a minimum at this time and started to rise afterward. During increasing spring discharge, both water temperature and EC reached their maximums, demonstrating that the water discharged at Glarey spring at that time was not freshly infiltrated glacial meltwater, but displaced water from the aquifer. Maximum spring discharge occurred ca. 10.5 h after the air temperature maximum, while minimum EC was observed after 18 h. Low values of EC indicate a high relative contribution of freshly infiltrated glacial meltwater (confirmed by low water temperatures, although the temperature minimum is less pronounced). The time shift between maximum spring discharge and minimum EC consequently demonstrates that the hydraulic connection between the glacier and the spring consists of a combination between pressure transfer and physical transport of meltwater. The calculated carbon sink is largely parallel to spring discharge. During the 3-day monitoring period, it varied between ca. 450 and

550 mmol/s and reached its daily maximum during maximum spring discharge.

Table 4 presents a complete statistical analysis of all data from the melting season. The mean discharge during this period is 1,001 L/s (higher than the annual average) and the mean bicarbonate concentration is 93.8 mg/L (lower than the annual average, see Table 2), thus resulting in a mean carbon sink of 701 mmol/s. The highest calculated value of carbon sink also occurs during the melting season, 1,583 mmol/s.

Discussion

It has been known for a long time that karst processes, i.e., the dissolution of carbonate minerals, act as an atmospheric sink for CO₂ and that the efficiency of this sink depends on several factors, such as temperature, precipitation, soil and vegetation (Yuan 1997; Liu and Zhao 2000; Gombert 2002; Liu et al. 2010). However, this paper presents the first detailed study of hydrochemical and hydrological variations along with the resulting variability of the atmospheric CO₂ sink in a glaciated karst area at high temporal resolution.

Due to the low temperature and the lack of soil and vegetation in glaciated areas, CO₂ partial pressures in the aquifer are generally low, which limits karst processes. At the main spring (Glarey) draining the Tsanfleuron glacier and karst aquifer system, the mean pCO₂ is 87.6 Pa or 876 ppmv (parts per million by volume; see Table 2), which is about 7 and 17 times lower than those observed in subtropical (Maolan, China) and tropical climate (Nongla, China) (Liu et al. 2007), respectively. This shows the importance of climate and land cover in controlling CO₂ partial pressures in aquifer.

Glarey spring shows significant seasonal and diurnal variations of discharge and electrical conductivity (EC),

Fig. 4 Seasonal variations of air temperature and precipitation, discharge and physicochemical parameters at Glarey spring, and calculated variability of CO_2 partial pressure, SIc and carbon sink

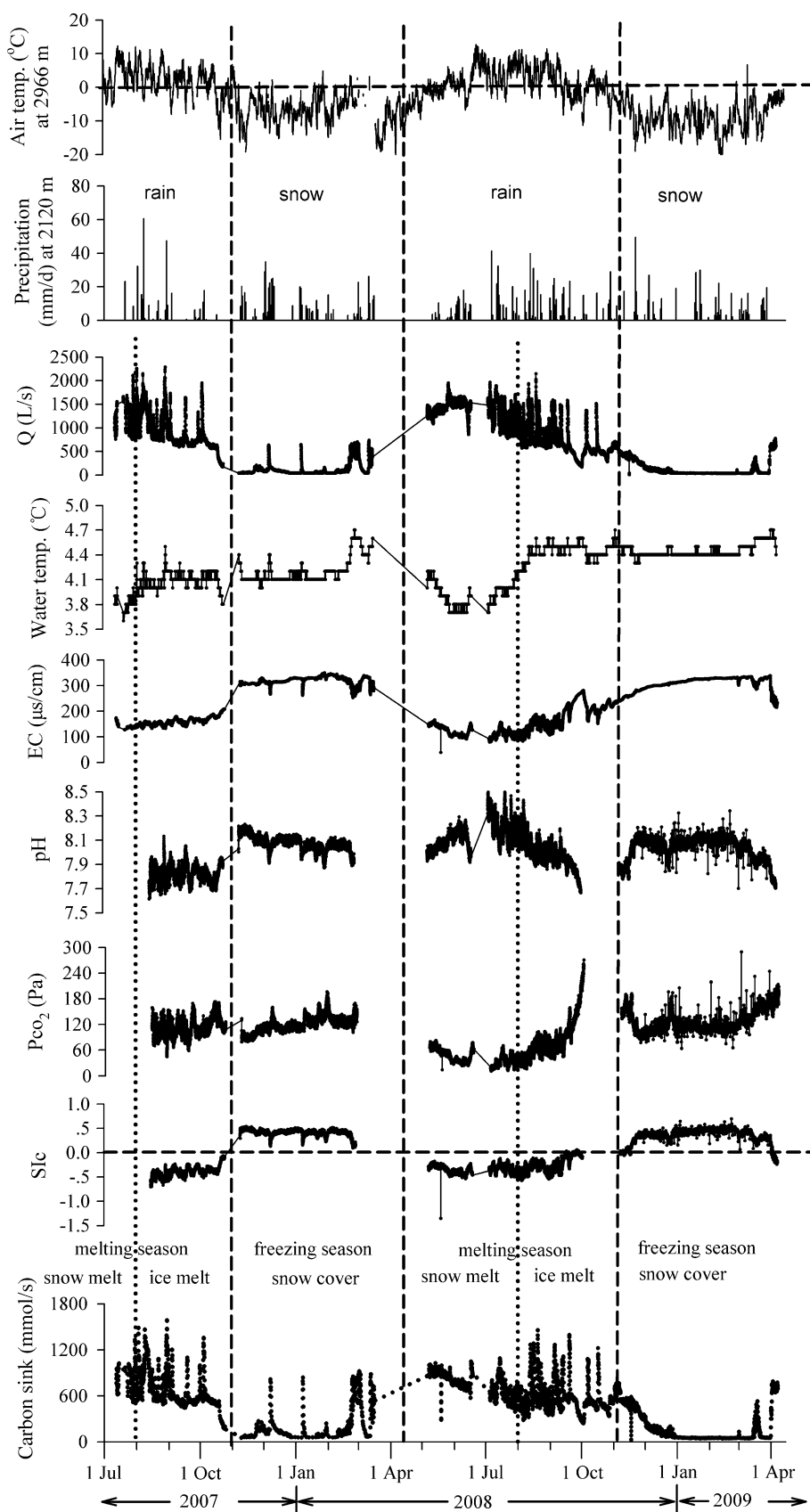


Fig. 5 Records of observed air temperature at 2,966 m, discharge of the Glarey spring, water temperature, electrical conductivity (EC) and pH, along with calculated values of CO₂ partial pressure, SIc and carbon sink at 30-min intervals under permanent freezing conditions, January 1–3, 2008

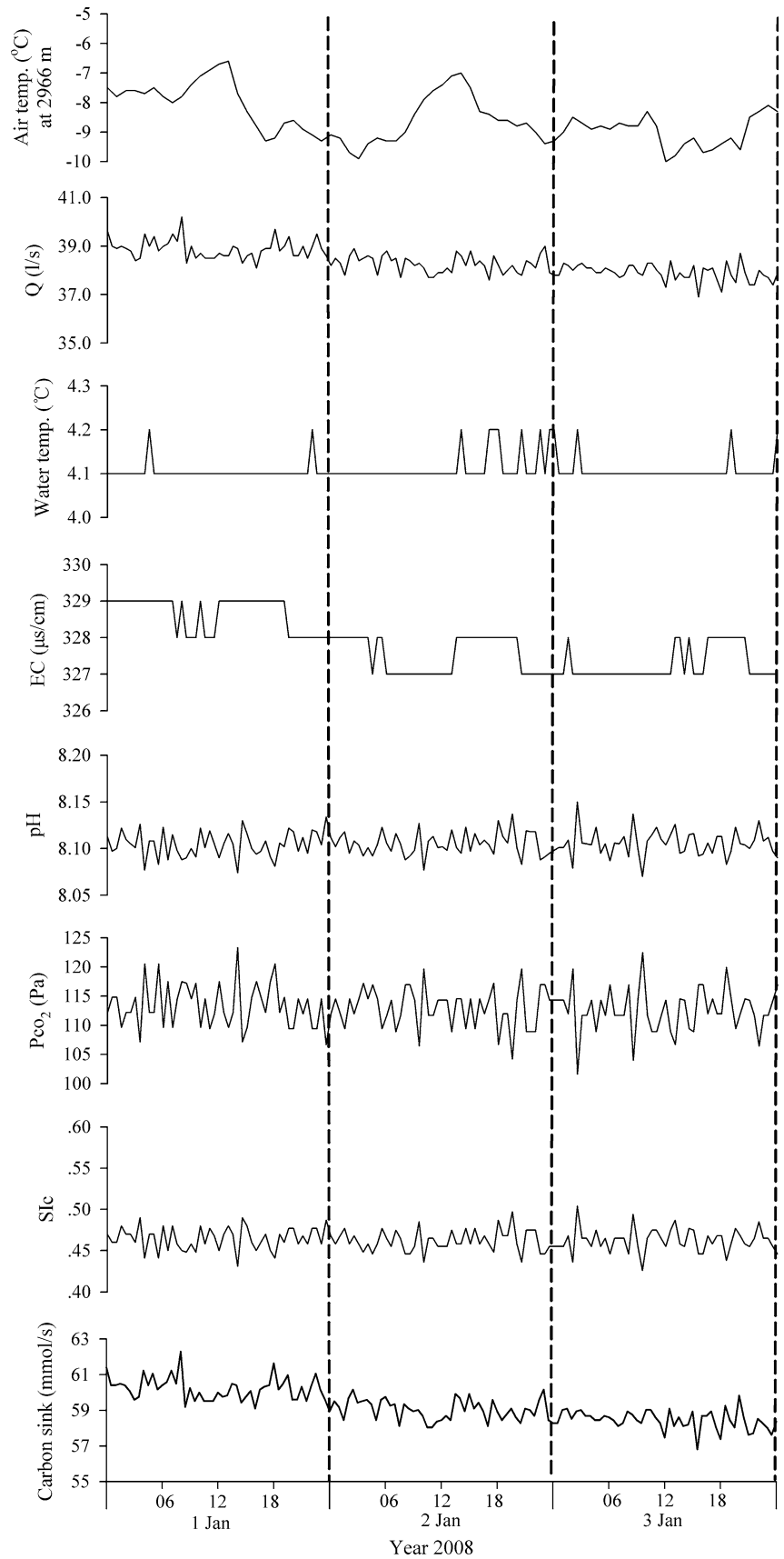


Table 3 Statistics on the hydrological and hydrochemical variation of Glarey spring during the freezing season (1 November 2007 through 15 April 2008)

	Air <i>T</i> (°C)	Discharge (L s ⁻¹)	Water <i>T</i> (°C)	EC (μS cm ⁻¹)	[Ca ²⁺] (mg L ⁻¹)	[HCO ₃ ⁻] (mg L ⁻¹)	pH	SI _C	pCO ₂ (Pa)	Carbon sink (mmol s ⁻¹)
<i>N</i>	4,008	6,165	6,165	6,165	6,165	6,165	5,318	5,318	5,318	6,165
Minimum	-20.3	35	4.02	252	45.3	141.3	7.87	0.04	75.7	50
Maximum	6.8	735	4.70	349	61.0	188.7	8.23	0.46	184.9	922
ED	27.1	700	0.69	97	15.8	47.4	0.36	0.42	109.2	872
Mean	-6.8	118	4.21	319	56.1	173.8	8.07	0.33	114.0	161
SD	4.6	142	0.15	16	2.6	7.8	0.06	0.07	17.2	181
CV	N/A	1.20	0.04	0.05	0.05	0.04	0.01	N/A	0.15	1.12

For legends, see Table 1

the latter being perfectly correlated to bicarbonate concentration. On a seasonal time scale, discharge and EC show clearly reversed variations: discharge is lowest during the freezing season and highest during the melting season, while EC is highest during the freezing season but lowest during the melting season (Fig. 4). According to Eq. 5, the carbon sink is proportional to a product of bicarbonate concentration (derived from EC) and discharge. Comparison of the mean values of these parameters during the freezing season (Table 3) and during the melting season (Table 4) reveals that discharge varies by a factor of 8.48, while EC varies in the opposite direction but only by a factor of 1.85. The effect of discharge variations consequently overrides the effect of EC variations. Therefore, the calculated carbon sink is largely parallel to discharge and varies by a factor of 4.34, with high values during the melting season and low values in winter. The mean carbon sink during the melting season is 701 mmol/s, while it is only 161 mmol/s in the freezing season.

This is consistent with findings by Hodson et al. (2000), who showed that specific annual discharge was the most significant control upon chemical denudation and transient CO₂ drawdown in glacierized basins, and basin lithology was an important secondary control, with carbonate-rich lithology showing the greatest chemical denudation rates and CO₂ drawdown.

Significant and regular diurnal variations of all parameters have been observed at the Glarey spring during the melting season, occasionally interrupted by rainfall events that create superimposed irregular variations. Diurnal variations of discharge and EC monitored at the spring are not in phase with air temperature, but display time shifts of several hours, reflecting the delayed response of glacial melt on temperature and the combined effect of pressure transfer and advective water transport from the glacier to the spring (Fig. 6). The calculated carbon sink also shows marked diurnal variations and is largely parallel to spring discharge.

The calculated mean annual carbon flux monitored at Glarey spring is 462 mmol/s. According to tracer test results obtained by Gremaud et al. (2009), the recharge area of the spring is approximately 10.9 km² large (Fig. 2). Based on the simplified assumption that the system behaves like a natural lysimeter (i.e., all recharge water goes to the spring), it is possible to estimate the mean carbon sink intensity of the studied glacier and karst system: 0.51 g km⁻² s⁻¹ or 16.08 t km⁻² a⁻¹. This corresponds to a CO₂ sink of 58.96 t km⁻² a⁻¹ and a limestone (calcite) denudation rate of 134 t km⁻² a⁻¹, very similar to that (133 t km⁻² a⁻¹) obtained by Singh and Hasnain (1998) in a high-altitude river basin on Garhwal Himalaya with similar lithology.

Taking into account the density of calcite (2.7 g/cm³), the calculated limestone denudation rate can also be expressed as ca. 50 mm/ka (1 ka = 1,000 years), which is three times higher than the world average (Hu et al. 1982) and rather unexpected for a cold climate and scarce soil and vegetation. The calculated CO₂ sink by karst processes in the Tsanfleuron glaciated karst system was three to nine times higher than that (5.72–13.93 t km⁻² a⁻¹) for an ice-free polar karst catchment: Londonelva, Svalbard (Krawczyk and Petterssons 2007).

The main reason for this higher CO₂ sink in the glaciated catchment is the larger and longer increase of spring discharge, because the relatively short snowmelt period is complemented and followed by a prolonged period of glacier melt (Hodgkins et al. 1997). During periods of glacier retreat, there is a transient surplus of meltwater resulting from the disequilibrium between ablation and accumulation. Gremaud and Goldscheider (2010) estimated that this transient meltwater quantity corresponds to ca. 20–35 % of the discharge of Glarey spring. This finding has implication for understanding the karst process-related atmospheric CO₂ sink in glaciated areas: this sink increases with increasing runoff caused by global warming, as also demonstrated by Krawczyk and Bartoszewski (2008) for the Scottbreen Basin, Svalbard.

Fig. 6 Records of observed air temperature at 2,966 m, discharge of the Glarey spring, water temperature, electrical conductivity (EC) and pH, along with calculated values of CO₂ partial pressure, SIc and carbon sink at 30-min intervals under the melting season conditions, 13–15 September 2007

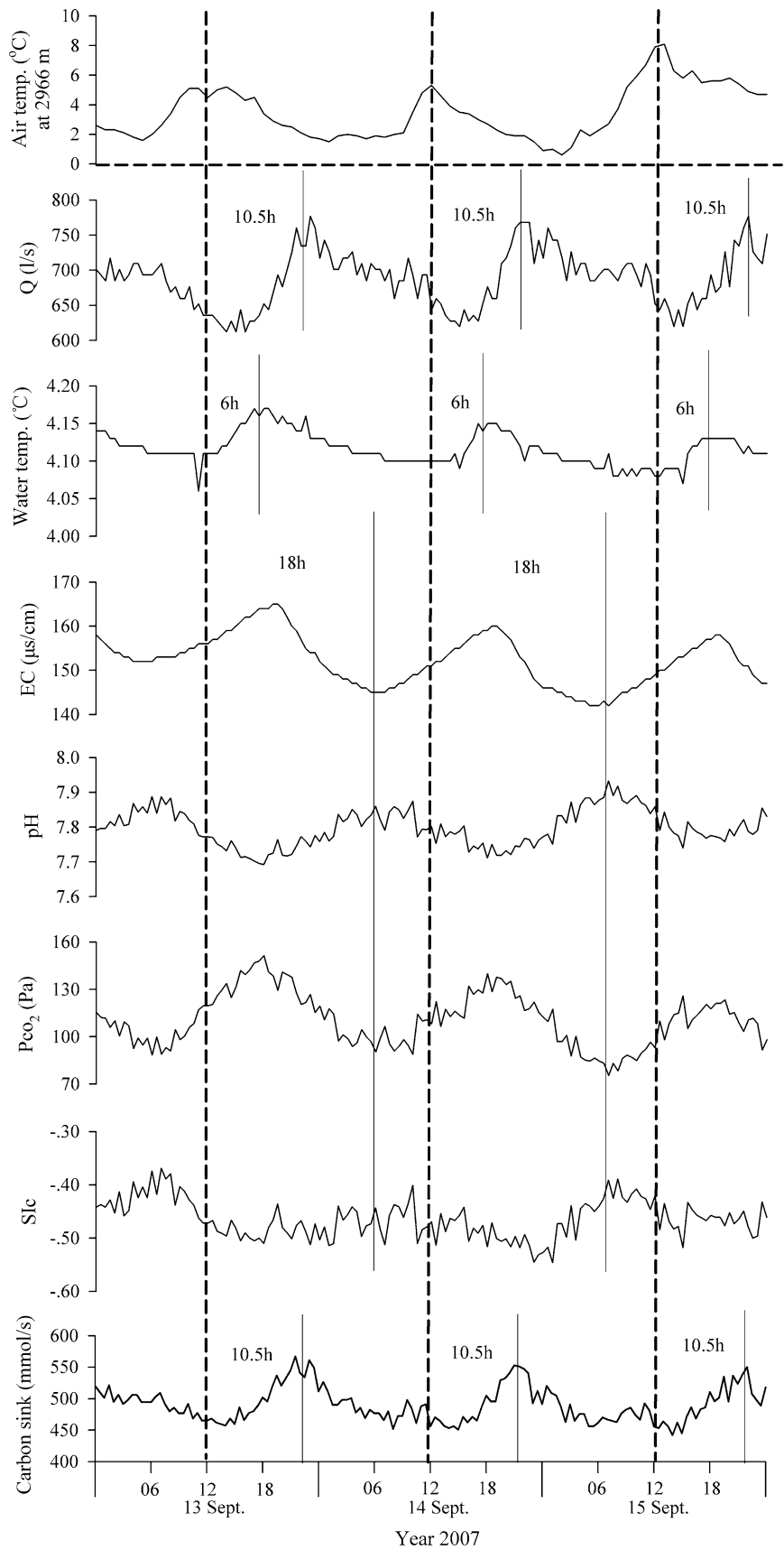


Table 4 Statistics on the variation of Glarey spring during the melting season (15 April 2008 through 1 November 2008)

	Air <i>T</i> (°C)	Discharge (L s ⁻¹)	Water <i>T</i> (°C)	EC (μS cm ⁻¹)	(Ca ²⁺) (mg L ⁻¹)	(HCO ₃ ⁻) (mg L ⁻¹)	pH	SI _C	pCO ₂ (Pa)	Carbon sink (mmol s ⁻¹)
<i>N</i>	4,776	7,750	7,750	7,750	7,750	7,750	6,328	6,328	6,328	7,750
Minimum	-14.7	162	3.68	38	10.5	36.8	7.66	-0.96	13.0	205
Maximum	12.8	2,145	4.64	281	50.0	155.5	8.53	0.00	260.6	1,583
ED	27.5	1,983	0.96	243	39.5	118.7	0.86	0.96	247.6	1,378
Mean	1.2	1,001	4.21	155	29.5	93.8	8.07	-0.26	65.5	701
SD	4.5	442	0.28	50.39	8.2	24.6	0.14	0.09	39.8	231
CV	N/A	0.44	0.07	0.33	0.28	0.26	0.02	N/A	0.61	0.33

For legends, see Table 1

Conclusions

For the first time, the atmospheric CO₂ sink at a glaciated alpine karst system (Tsanfleuron, Switzerland) has been investigated by means of high-resolution monitoring of hydrochemical variations during about two complete hydrological years.

It was found that there were clear seasonal and diurnal hydrochemical variations, which were controlled chiefly by air temperature, the latter influencing the recharge to the karst aquifer by snow and glacier melt. The rate of the atmospheric CO₂ sink depends on two parameters that are inversely correlated to each other: discharge and bicarbonate concentration. The CO₂ sinks were found to be more than four times higher in the melting season than in the freezing season, because the effect of higher flow rates overrides the effect of lower concentrations. During the melting season, significant hydrological and hydrochemical variations were also observed on a diurnal time scale, with maximum CO₂ sinks occurring during maximum flow rates.

This finding has implication for understanding the atmospheric CO₂ sink in glaciated areas consisting of karstified carbonate rocks or other rock types including carbonate minerals: the carbon sink increases during periods of increasing meltwater production, i.e., periods of glacier retreat. This means that carbonate weathering in glaciated areas may act as a regulator for atmospheric CO₂ and provide a negative climate feedback mechanism that partly counteracts the anthropogenic increase of atmospheric CO₂. However, this is a transient effect that is most effective when the meltwater production is highest, i.e., in the case of large glaciers that retreat quickly. If glacier retreat continues at the current rate, the Tsanfleuron glacier and many other small glaciers will disappear within a few decades, so that the described regulation effect will also decrease.

Acknowledgments This study was funded by the Swiss National Science Foundation (project GLACIKARST, grant no 200020-121726/1),

the Hundred Talents Program of Chinese Academy of Sciences (CAS), the foundation of the CAS for Innovation (Grant No.kzcx2-yw-306) and the National Natural Science Foundation of China (Grant No. 40872168).

References

- Anderson SA, Drever JI, Humphrey NF (1997) Chemical weathering in glacial environments. *Geology* 25:399–402
- Brown GH, Tranter M, Sharp MJ, Gurnell AM (1994) The impact of post mixing chemical reactions on the major ion chemistry of bulk meltwaters draining the Haut Glacier d' Arolla, Valais, Switzerland. *Hydrol Process* 8:465–480
- Drever JI (1988) The geochemistry of natural waters. Englewood Cliffs, Prentice-Hall, p 437
- Fairchild IJ, Bradby L, Sharp M, Tison JL (1994) Hydrochemistry of carbonate terrains in alpine glacial settings. *Earth Surf Process Landf* 19:33–54
- Fairchild IJ, Killawee JA, Sharp MJ, Spiro B, Hubbard B, Lorrain RD, Tison JL (1999) Solute generation and transfer from a chemically reactive alpine glacial-proglacial system. *Earth Surf Process Landf* 24:1189–1211
- Gibbs MT, Kump LR (1994) Global chemical erosion during the last glacial maximum and the present: sensitivity to changes in lithology and hydrology. *Paleoceanography* 9:529–543
- Goldscheider N (2005) Fold structure and underground drainage pattern in the alpine karst system Hochifen–Gottesacker. *Ecolgae Geol Helv* 98:1–17
- Gombert P (2002) Role of karstic dissolution in global carbon cycle. *Global Planet Change* 33:177–184
- Gremaud V, Goldscheider N, Savoy L, Favre G, Masson H (2009) Geological structure, recharge processes and underground drainage of a glacierised karst aquifer system, Tsanfleuron–Sanetsch, Swiss Alps. *Hydrogeol J* 17:1833–1848
- Gremaud V, Goldscheider N (2010) Geometry and drainage of a retreating glacier overlying and recharging a karst aquifer, Tsanfleuron–Sanetsch, Swiss Alps. *Acta Carsologica* 39:289–300
- Hodgkins R, Tranter M, Dowdeswell JA (1997) Solute provenance, transport and denudation in a High Arctic glacierized catchment. *Hydrol Process* 11:1813–1832
- Hodson A, Tranter M, Vatne G (2000) Contemporary rates of chemical denudation and atmospheric CO₂ sequestration in glacier basins: an arctic perspective. *Earth Surf Process Landf* 25:1447–1471
- Holland HD (1978) The chemistry of atmospheres and oceans. Wiley, New York, p 351
- Hu M, Stallard RF, Edmond JM (1982) Major ion chemistry of some large Chinese rivers. *Nature* 298:550–553

- Krawczyk WE, Pettersson L (2007) Chemical denudation rates and carbon dioxide drawdown in an ice-free polar karst catchment: Londoneiva, Svalbard. *Permafrost Periglacial Process* 18:337–350
- Krawczyk WE, Bartoszewski SA (2008) Crustal solute fluxes and transient carbon dioxide drawdown in the Scottbreen Basin, Svalbard in 2002. *J Hydrol* 362:206–219
- Liu Z, Zhao J (2000) Contribution of carbonate rock weathering to the atmospheric CO₂ sink. *Environ Geol* 39:1053–1058
- Liu Z, Groves C, Yuan D, Meiman J, Jiang G, He S (2004) Hydrochemical variations during flood pulses in the southwest China peak cluster karst: impacts of CaCO₃–H₂O–CO₂ interactions. *Hydrological Process* 18:2423–2437
- Liu Z, Li Q, Sun H, Wang J (2007) Seasonal, diurnal and storm-scale hydrochemical variations of typical epikarst springs in subtropical karst areas of SW China: soil CO₂ and dilution effects. *J Hydrol* 337:207–223
- Liu Z, Dreybrodt W, Wang H (2010) A new direction in effective accounting for the atmospheric CO₂ budget: considering the combined action of carbonate dissolution, the global water cycle and photosynthetic uptake of DIC by aquatic organisms. *Earth Sci Rev* 99:162–172
- Sharp MJ, Tranter M, Brown GH, Skidmore M (1995) Rates of chemical denudation and CO₂ drawdown in a glacier-covered Alpine catchment. *Geology* 23:61–64
- Singh AK, Hasnain SI (1998) Major ion chemistry and weathering control in a high altitude basin: Alaknanda River, Garhwal Himalaya, India. *Hydrological Sci J* 43:825–843
- Stumm W, Morgan JJ (1981) *Aquatic chemistry*. Wiley-Interscience, New York, p 780
- Tranter M, Brown GH, Raiswell R, Sharp MJ, Gurnell AM (1993) A conceptual model of solute acquisition by Alpine glacial meltwaters. *J Glaciol* 39:573–581
- Wigley TML (1977) WATSPEC: a computer program for determining equilibrium speciation of aqueous solutions. *Br Geomorphol Res Group Tech Bull* 20:1–48
- Yuan D (1997) The carbon cycle in karst. *Zeitschrift für Geomorphologie* 108:91–102